Phys. Status Solidi B **252,** No. 1, 170–180 (2015) / **DOI** 10.1002/pssb.201451065

physica status solidi b
www.pss-b.com
basic solid state physics

Evaluation of the characteristic curves of a-Si:H based devices with the Simmons–Taylor approximation when the defect pool model is used

Marcelo G. De Greef* **and Francisco A. Rubinelli****

INTEC, Universidad Nacional del Litoral, Güemes 3450, 3000 Santa Fe, Argentina

Received 20 February 2014, revised 4 July 2014, accepted 4 July 2014
Published online 13 August 2014

Keywords defect pool model, hydrogenated amorphous silicon, optical detectors, Simmons–Taylor approximation, solar cell modeling

* Corresponding author: e-mail mdegreef@santafe-conicet.gov.ar, Phone: +54 342 455 9175, Fax: +54 342 450 944
** e-mail frubinelli@santafe-conicet.gov.ar, Phone: +54 342 455 9175, Fax: +54 342 450 944

The performance of a-Si:H devices is highly sensitive to the density of gap states: tail states are distributed in two exponentials and defect states are generated by dangling bonds (DB). The density of DB in a-Si:H can be evaluated with the defect pool model (DPM). Charge trapping and recombination of electron–hole pairs through tail states are described by the Shockley–Read–Hall (SRH) formalism while defect states behave as amphoteric. Equations derived with the SRH formalism can be simplified with the Simmons–Taylor's approximation (STA), especially with the "0 K" approximation (0KSTA). Amphoteric-like defect states were approximated by donor- and acceptor-like decoupled states (DSA). The accuracy of STA was tested in a-Si:H based devices when the density of DB is evaluated with the DPM for different illumination conditions, voltages, temperatures, and some key electrical parameters. Our code was modified to include both the STA and the DSA. Our results indicate that the STA is very accurate under illuminated conditions. Under dark conditions, the STA is acceptable for forward voltages but overestimates the dark current at reverse voltages. The 0KSTA can be used under illuminated conditions for any applied voltage and under dark conditions for forward voltages.

1 Introduction The performance of hydrogenated amorphous silicon (a-Si:H) based electronic devices is highly dependent on the density of states present in the band gap. The density of states in these materials contains two exponentially decreasing tails connected to the bands and a considerable number of defect states. Charge trapping and recombination of electron–hole pairs through gap states are very often described by the Shockley–Read–Hall (SRH) formalism.

In a previous contribution, the current voltages (J–V) and spectral responses (SR) characteristic curves of a-Si:H and μc-Si:H devices were evaluated by modeling charge trapping and recombination with three different approaches: the SRH formalism, the Simmons–Taylor's approximation (STA) and the so called "0 K" Simmons–Taylor's approximation (0KSTA) [1]. In the last case, the occupation functions and the recombination rate are represented by step functions that abruptly change at the trapped quasi-Fermi levels defined by Simmons and Taylor [2]. The J–V and SR curves obtained with the three formalisms were compared under different scenarios: dark and different illuminated conditions, forward and reverse bias voltages, lower and higher temperatures, thin and thick intrinsic layers, and for different key electrical parameters like the mobility gap in order to cover different devices based in thin films of a-Si:H and its alloys. Our results indicated that the STA was an acceptable approximation of the SRH model when the device is working under illumination. Under dark conditions, the STA was suitable when the device was forward biased but slightly overestimated the dark current when the device was reversed biased. The 0KSTA under illuminated conditions or under dark conditions for forward voltages the 0KSTA was also a reasonable approximation with some few exceptions like junctions with low gap intrinsic layers. The 0KSTA cannot be applied when the device was reversed biased and operates under dark conditions. In our

contribution, the density of defect states or dangling bonds (DB) was assumed to be uniform within each device layer and represented by pairs of single occupied acceptor-like and donor-like states. The uniformity of the density of DB was recognized in our paper as the Uniform density of states model (UDM) and the representation of DB as a pairs of acceptor and donor states as the decoupled state approximation (DSA).

In this paper, the accuracy of the STA and 0KSTA in a-Si:H based devices is now tested evaluating the density of DB with the defect pool model (DPM). This issue was not covered in our previous contribution due to its inherent complexity and an excessive extension of our manuscript. Although fittings of characteristics *J–V* and spectral responses (SR) of a-S:H devices can be achieved with either the DPM or the UDM, the DPM is widely used in a-S:H devices because it can successfully capture experimentally trends while the UDM could give rise to predictions in contradiction with some experimental findings [3, 4].

The DPM is based in an elaborated thermodynamic approach where the creation of defects is described through specific microscopic reactions that involve the breaking of weak Si–Si bonds (WB) stabilized by diffusive hydrogen motion and also the breaking and reforming of Si–H bonds. Hydrogen passivation of the newly created DB prevents back-transformation into a WB. Hence, the charge state of a DB after bond-breaking influences the final equilibrium of the electron configuration. Therefore, the position of the Fermi level in the mobility gap influences the equilibrium DB concentration that is computed by minimizing the free energy of the system composed by WB, DB, and H bonds. The equilibrium density of DB reached at the freezing temperature depends of the Fermi energy. Hence, the predicted density of DB is highly non-uniform along the intrinsic layer of a-Si:H p–i–n devices being considerable higher near the p/i and i/n interfaces than in the bulk [5].

It is important to emphasize that the derivation of the density of DB in the DPM assumes that defect states associated with Si–Si bonds have an amphoteric character [6, 7]. On the other hand, the STA was derived for decoupled states (acceptor-like and donor-like states). Hence, the trapped charge concentrations and the recombination rate expressions obtained with the DPM for amphoteric states must first be re-written for decoupled states. In order to test the validity of the STA in a-Si:H based devices modeled with the DPM, two approximations have to be simultaneously tested: the DSA in the non-uniform density of DB predicted by the DPM and the STA itself once the DSA was applied to the original equations of the DPM.

In this paper, the density of DB will be evaluated with the DPM. At the deposition or freezing temperature, the material is assumed to reach the state of thermodynamic equilibrium. In the derivation of the DB density of the DPM the amphoteric nature of DB is taken into account. Therefore, the occupation functions F_{eq}^{+}, F_{eq}^{0}, and F_{eq}^{-} for amphoteric states at thermodynamic equilibrium were used by Powel and Deane [7] (Eqs. (5)–(7), p. 10815 of this reference). The device operates out of equilibrium conditions at lower temperatures than the freezing temperature (for instance at room temperature). The DB profile evaluated with the DPM at the freezing temperature does not change during device operation (except for the possible Stabler Wronski effect). The trapped carrier concentrations and recombination rates under non-equilibrium conditions can be evaluated by modeling DB as either amphoteric or decoupled states. In the second case, some errors will be introduced. To our knowledge, the Simmons–Taylor approximation was derived only for decoupled states. Hence, the non-equilibrium occupation functions f^{+}, f^{0}, and f^{-} of amphoteric states should first be approximated by the occupation functions f and $1-f$ of the SRH formalism for donor- and acceptor-like states (Section 4).

Kron and van Swaaij [8] have studied in detail the ideality factor of dark *J–V* curves of a-Si:H p–i–n diodes modeling the DB density with the DPM. In their papers, they used the 0 K Simmons–Taylor approximation that considerably simplified the interpretation of their results (see their references in [8]) They have reached interesting conclusions but we could not find in the literature a paper where the use of the 0 K Simmons–Taylor approximation was justified when the DPM was adopted to evaluate the DB density in a-Si:H devices. This paper is an attempt to fill this void.

Our paper is organized as follows: in Section 2, our methodology is briefly described, in Section 3, the DPM is presented, in Section 4, the implementation of the DSA that describes charge trapping and recombination within the DPM is discussed, and in Section 5, the predictions obtained with the STA and the 0KSTA are compared with the ones obtained with the DPM where DB are modeled with amphoteric states. Finally in our conclusions, the main results are summarized.

2 Methodology The device structure that was analyzed is as follows: TCO/p-a-SiC:H/i-a-Si:H/n-a-Si:H/Al with a 5-nm thick buffer layer between the p- and i-layers. The front contact is an Asahi U-type (employing textured SnO_2:F). The p- and n-layer thicknesses are 10 and 20 nm thick, respectively. Our data correspond to a-Si:H based p–i–n junctions with intrinsic layer thicknesses of 200 and 600 nm. Both devices are in the annealed state and were characterized at Delft University of Technology.

The experimental *J–V* characteristics of the a-Si:H based p–i–n devices were fitted in order to calibrate the input parameters of our computer code D-AMPS described elsewhere [9]. The density of DB was evaluated with the DPM inside the intrinsic and buffer layers. The density of DB in the doped layers was assumed to be uniform but the number of defects enclosed in the D^{+}, D^{0}, and D^{-} Gaussians are given by the DPM. We adopted $D^{+} \gg D^{0} \gg D^{-}$ and $D^{+} \ll D^{0} \ll D^{-}$ in the p- and n-layers, respectively, following the equations [21, 22] proposed by Powel and Deane [7] (see p. 10815 of this reference). The optical parameters were obtained from reflection and transmission spectra measured on layers deposited on glass. The global

density of states and the Urbach slope were extracted using dual beam photoconductivity. The correlation energy U was assumed equal to 0.2 eV [6, 7]. The freezing temperature was set to 460 K [10]. The hydrogen concentration was adopted equal to 1×10^{21} cm^{-3} [6]. The parameters used to match the experimental data are listed in Table 1. The optical model was briefly described in previous publications [1].

Figures 1 and 2 show our fittings of the dark and the light J–V characteristics measured at 40 °C and at room temperature, respectively. The light source corresponds to AM1.5 illumination. In our fittings of Figs. 1 and 2, the carrier trapping and the recombination rate were evaluated with the full expressions of the DPM without making any approximations. DB were modeled as amphoteric states at both the freezing and the operating temperature of the device.

3 The defect pool model States associated to DB show an amphoteric character: i.e., they can act as either donor-like or acceptor-like, depending on their charge state.

Table 1 Setting parameters.

parameters	p	i	n
W (nm)	10	200/600	20
E_G (eV)	1.9	1.72	1.72
G_{A0} G_{D0} (cm^{-3} eV^{-1})	1×10^{21}	1×10^{21}	1×10^{21}
N_c, N_v (cm^{-3})	3×10^{20}	3×10^{20}	3×10^{20}
μ_N (cm^2 V^{-1} s^{-1})	5	20	5
μ_P (cm^2 V^{-1} s^{-1})	1	4	1
E_D (meV)	80	44	50
E_A (meV)	25	30	30
t_N^+ t_P^- (cm^2)	1×10^{-15}	1×10^{-15}	1×10^{-15}
t_N^0 t_P^0 (cm^2)	1×10^{-17}	1×10^{-17}	1×10^{-17}
D^- (cm^{-3})	3.04×10^{12}	–	6.78×10^{18}
D^0 (cm^{-3})	2×10^{16}	–	1.6×10^{15}
D^+ (cm^{-3})	5.25×10^{18}	–	1.51×10^{12}
E_D^- (eV)	0.7	–	0.6
E_D^0 (eV)	1	–	0,9
E_D^+ (eV)	1.3	–	0.12
σ_D (eV)	0.13	–	0.13
E_{DP} (eV)	–	1.03/1.1	–
Δ_{DP} (eV)	–	0.295	–
σ_N^+ σ_P^- (cm^2)	1×10^{-14}	1×10^{-14}	1×10^{-14}
σ_N^0 σ_P^0 (cm^2)	2×10^{-16}	1×10^{-16}	2×10^{-16}

List of electrical input parameters obtained from fitting the dark and light J–V curves. The meaning of the symbols is as follows: W is the layer thickness, E_G is the mobility gap, G_{A0} and G_{D0} are the density of states at the conduction and valence band edges, respectively, N_c and N_v are the effective density of states at the conduction and valence bands, respectively, μ_N and μ_P are the electron and hole mobilities, E_D and E_A are the valence and conduction tail slopes, t_N^0 and t_P^- are the cross-sections for electrons and holes at acceptor tail states, t_N^+ and t_P^0 are the cross-sections for electrons and holes at donor tail states, D^-, D^0, and D^+ are the defect densities enclosed by each Gaussian, E_D^-, E_D^0, and E_D^+ are the peak positions of Gaussians referred to the valence band edge, σ_D are the standard deviations, E_{DP} is the peak energy of defect pool, Δ_{DP} is the separation between the positive charge in a-Si:H n-layers and the negative charge in a-Si:H p-layers, and σ_N and σ_P are the defect states cross-sections for electrons an holes. The superscript +, 0, and − indicates the charge status of the traps. The thermal velocity v_{TH} was assumed as 107 cm s^{-1} for both electrons and holes.

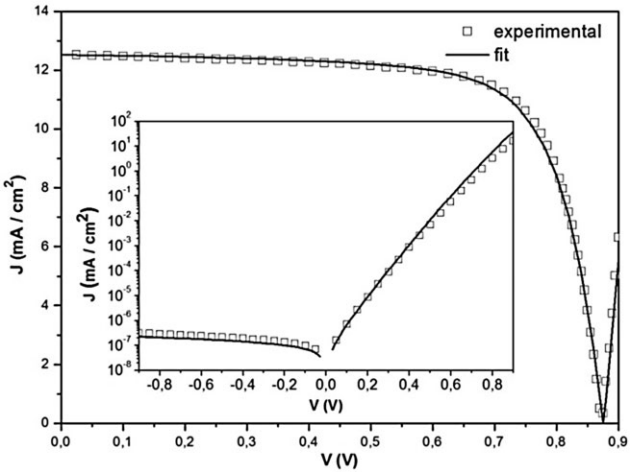

Figure 1 Fitting of the experimental dark and light J–V characteristics of an a-Si:H based p–i–n junction with a 200 nm thick intrinsic layer. The density of DB is modeled with the DPM.

Amphoteric DB can adopt three different charge status: positive (+), neutral (0), or negative (−) when they are occupied by zero, one, or two electrons, respectively. The theory for multiple charge levels was developed by Sah and Shockley [11]. The amphoteric state is represented by two energy levels: $E^{+/0}$ associated to the +/0 transition and $E^{0/-}$ associated to the 0/− transition. In these two levels, the four processes of electron or hole capture and emission can take place. The two levels are separated by the energy U. Assuming that D denotes a DB state and its superscript gives the charge status, the possible transitions are listed in Table 2.

The formalism of amphoteric states will be recognized in this contribution with the initials AMP. The mathematical expressions for the occupation functions of the three charge

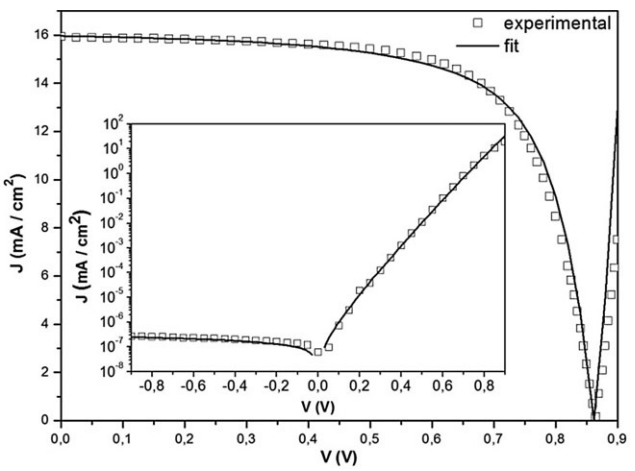

Figure 2 Fitting of the experimental dark and light J–V characteristics of an a-Si:H based p–i–n junction with a 600 nm thick intrinsic layer. The density of DB is modeled with the DPM.

Table 2 Capture and emission processes in a three-state amphoteric level.

$E^{+/0}$ process	rate		$E^{0/-}$ process	rate	
electron capture	r_1	$D^+ + e \rightarrow D^0$	electron capture	r_5	$D^0 + e \rightarrow D^-$
electron emission	r_2	$D^0 \rightarrow e + D^+$	electron emission	r_6	$D^- \rightarrow e + D^0$
hole capture	r_3	$D^0 + h \rightarrow D^+$	hole capture	r_7	$D^- + h \rightarrow D^0$
hole emission	r_4	$D^+ \rightarrow h + D^0$	hole emission	r_8	$D^0 \rightarrow h + D^-$

states, the trapped carrier densities and the recombination rate under steady-state non-equilibrium conditions have been derived by different authors [11–13]. Under steady state conditions, the rates of Table 2 must fulfill the following two equations:

$$r_2 + r_3 - r_1 - r_4 = 0, \tag{1a}$$

$$r_5 + r_8 - r_6 - r_7 = 0. \tag{1b}$$

Using (1), the principle of detailed balance, and the condition that the sum of the occupation probabilities of having one state unoccupied, singly occupied and doubly occupied is unity the non-equilibrium occupation functions f^+, f^0, and f^- can be obtained [14, 15]. The average charge Q and the recombination efficiency η_R for one DB (i.e., the recombination per energy state E), can be derived as [16–18]:

$$Q(E) = q(f^+ - f^-), \tag{2a}$$

$$f^+ = \frac{P^0 P^-}{N^+ P^- + P^0 P^- + N^+ N^0},$$

$$f^0 = \frac{N^+ P^-}{N^+ P^- + P^0 P^- + N^+ N^0},$$

$$f^- = \frac{N^0 N^+}{N^+ P^- + P^0 P^- + N^+ N^0},$$

$$\eta_R(E) = r_1 + r_2 - r_5 - r_6, \tag{2b}$$

$$\eta_R(E) = v_{th}^2 (pn - n_i^2) \frac{\sigma_N^+ \sigma_P^0 P^- + \sigma_N^0 \sigma_P^- N^+}{N^+ P^- + P^0 P^- + N^+ N^0},$$

$$N^+ = n v_{th} \sigma_N^+ + e_P^+,$$

$$N^0 = n v_{th} \sigma_N^0 + e_p^0$$

$$P^- = p v_{th} \sigma_P^- + e_n^-,$$

$$P^0 = p v_{th} \sigma_P^0 + e_n^0,$$

where v_{th} is the thermal carrier velocity assumed identical for electrons and holes, n and p are the free electron and hole concentrations, respectively, n_i is the intrinsic carrier concentration, e_p^+ and e_p^0 are emission coefficients for holes at the $E^{+/0}$ and $E^{0/-}$ levels and e_n^- and e_n^0 are emission coefficients for electrons at the same levels, respectively. The symbol σ stands for the respective cross-sections for electrons and holes associated to the capture processes that oppose to the respective emission rates.

Powel and Deane [6] have derived in the DPM the following expression for the DB distribution:

$$N(E) = \gamma \left[\frac{2}{F_{eq}^0(E)} \right]^{kT/2E_D} P\left(E + \frac{\sigma_{DP}^2}{2E_D} \right), \tag{3}$$

where the coefficient γ is given by

$$\gamma = G_{D0} \left(\frac{H}{N_{SiSi}} \right)^{kT/4E_D} \left(\frac{2E_D^2}{2E_D - kT_F} \right) \times \exp\left(-\frac{1}{2E_D} \left[E_{DP} - E_v - \frac{\sigma_{DP}^2}{4E_D} \right] \right),$$

and the defect-pool function, $P(E)$ by

$$P(E) = \left(2\sigma_{DP}^2 \pi \right)^{-1/2} \exp\left(-\frac{(E - E_{DP})^2}{2\sigma_{DP}^2} \right).$$

In these equations, the meaning of symbols is as follows: T_F is the freezing temperature, E_D is the characteristic slope of the valence band tail, G_{D0} is the density of states at the valence band edge, N_{SiSi} is the total number of electrons in the silicon bonding states, E_{DP} is the energy of the peak of the defect pool, σ_{DP} is the width of the pool, and E_v is the valence band mobility edge. In Eq. (3), F_{eq}^0 is the equilibrium occupation function of neutral amphoteric defect states at the freezing temperature [5].

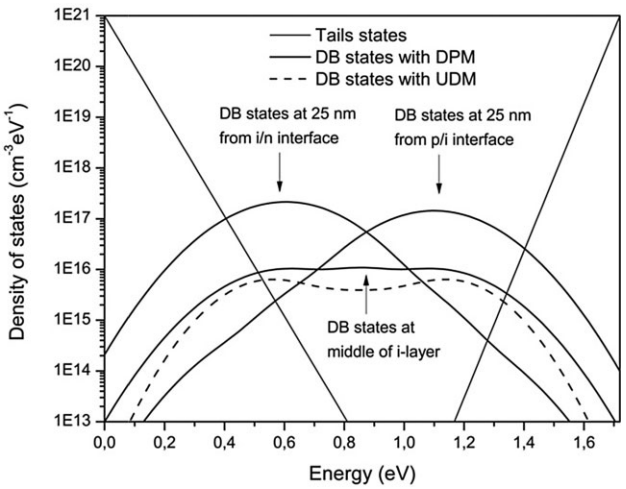

Figure 3 Density of gap states as predicted by the DPM inside a 600 nm thick intrinsic layer thickness of an a-Si:H p–i–n device. Three different x-locations in the i-layer are shown: near the p/i interface, at middle of the layer and near the i/n interface. Density of DB used in our previous contribution [1] where a uniform density of DB was adopted along the whole intrinsic layer is shown for comparison by dotted lines.

The main result of the DPM is that the defect distribution depends on the energy position of the Fermi-level relative to the band edges. Since this energy position changes with the spatial location inside the device the distribution of defect states also varies with the x-position. Figure 3 shows the defect distribution computed with Eq. (3) in three different regions of the intrinsic layer.

The total recombination rate R and the space-charge density ρ are evaluated by integrating the recombination efficiency and the average charge for each DB over all the gap states situated between the valence and conduction band mobility edges E_v and E_c:

$$R = \int_{E_v}^{E_c} N(E)\eta_R(E)\mathrm{d}E, \tag{4a}$$

$$\rho = \int_{E_v}^{E_c} N(E)Q(E)\mathrm{d}E, \tag{4b}$$

where $N(E)$ is the density of states obtained with Eq. (3). In (4), the non-equilibrium occupation functions f^+, f^0, and f^- are at the device temperature T and not at the freezing temperature (see Eqs. (2)).

4 The defect pool model with the decoupled state approximation The STA was derived in the literature only for decoupled states. Hence, the DSA should be previously implemented in (4) before applying the STA. The DSA consist in replacing the non-equilibrium occupation functions f^+, f^0, and f^- of (2) by the SRH occupation functions f and $1-f$ for electrons and holes, respectively. Expressions (2) for the average charge $Q(E)$ and the recombination efficiency $\eta_R(E)$ are modified by the DSA as [19]:

$$\eta_{Rd}(E) = v_{th}^2\sigma_N^+\sigma_P^0\frac{np - n_i^2}{nv_{th}\sigma_N^+ + pv_{th}\sigma_P^0 + e_n^0 + e_p^+}, \tag{5a}$$

$$\eta_{Ra}(E) = v_{th}^2\sigma_N^0\sigma_P^-\frac{np - n_i^2}{nv_{th}\sigma_N^0 + pv_{th}\sigma_P^- + e_n^- + e_p^0}, \tag{5b}$$

$$Q_d(E) = q(1 - f_d), \tag{5c}$$

$$Q_a(E) = qf_a, \tag{5d}$$

$$Q(E) = Q_d(E) - Q_a(E). \tag{5e}$$

Furthermore (4) can be rewritten as

$$R = \int_{E_v}^{E_c} [N_d(E)\eta_{Rd}(E) + N_a(E)\eta_{Ra}(E)]\mathrm{d}E, \tag{6a}$$

$$\rho = \int_{E_v}^{E_c} [N_d(E)Q_d(E) - N_a(E)Q_a(E)]\mathrm{d}E. \tag{6b}$$

The subscripts d and a refer to donor-like and acceptor-like states, respectively. In the DSA, DB are represented by pairs of donor and acceptor states. In particular when the DSA is used in the DPM, the density of DB $N(E)$, given by Eq. (3), has to be replaced by two densities: one of donor-like states $N_d(E)$ and other of acceptor-like states $N_a(E)$. $N_d(E)$ is a copy of $N(E)$ that should be placed $kT\ln(2)$ below (in energy) of $N(E)$ and $N_a(E)$ is another copy of the same density $N_d(E)$ that should be placed above of $N(E)$ (in energy) by $U + 2kT\ln(2)$ [7] as shown in Fig. 4. As F_{eq}^0 in Eq. (3) is part of the expression derived by Powel and Deane for the density $N(E)$ of DB in a-Si:H at the freezing temperature T_F the DSA was not applied to F_{eq}^0. Hence, the total recombination rate in the DSA is given by the sum of the recombination processes taking place in donor-like and acceptor-like states. This assumption tends to overestimate the recombination losses through neutral states [5]. When DB are modeled as amphoteric states they cannot simultaneously behave as donor-like and acceptor-like neutral states as in the decoupled approximation. The charge density is given by the difference between

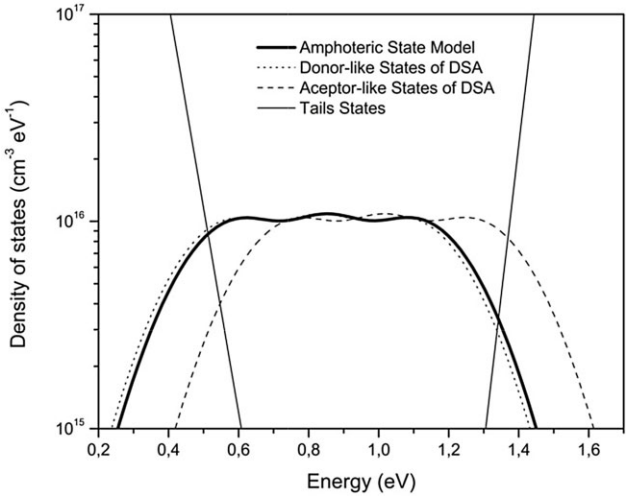

Figure 4 Distribution of DB with respect to the gap state energy inside the intrinsic layer of the p–i–n device at the middle of i-layer predicted with the defect pool model that takes into account their amphoteric character (solid line). In the decoupled state approximation, the density of donor-like states is given by the same distribution (solid line) slightly displaced by $kT\ln(2)$ to the left-hand side (dotted line) and the density of acceptor-like states is also given by the same distribution of DB but displaced in energy by $U + kT\ln(2)$ to the right-hand side (dashed line). Tail states are also shown using thinner solid lines.

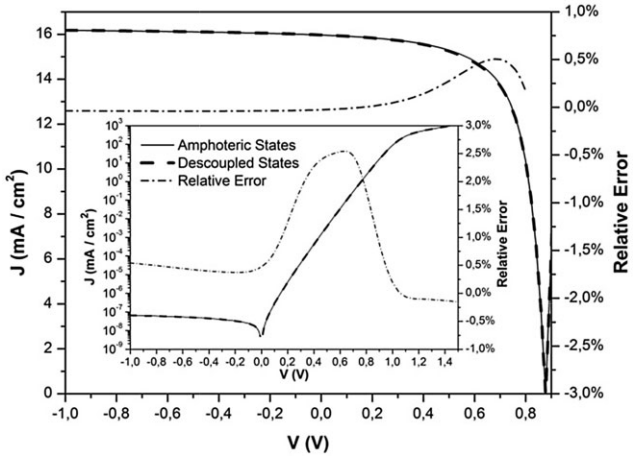

Figure 5 Predicted dark and light (AM1.5 illumination) *J–V* curves by D-AMPS for an a-Si:H based p–i–n device at room temperature using the DPM and modeling DB as either amphoteric or decoupled states. Relative errors are included. The intrinsic layer is 600 nm thick.

the positively charged donor-like states and the negatively charge acceptor-like states (5c). The errors introduced by this approximation have been already discussed in the literature for a uniform density of states [20]. Although there is a priori no reason to suspect that the DSA could fail when the density of DB is not uniform, the complexity of the algorithms developed by Powel and Deane makes this checking prudent. The two conditions to guarantee the accuracy of the DSA are fulfilled: the charged cross-sections are much higher than the neutral cross sections (100 times higher in the intrinsic layer and 50 times higher in doped layers as it can be seen in Table 1) and the correlation energy U is positive and considerably larger than kT ($U = 0.2\,\text{eV}$) [5]. However, as it was discussed in a previous publication [20], in computer modeling an error introduced in the recombination rate can affect the final free carrier concentrations and the gap-state occupation function values that would in turn alter the trapped carrier concentrations evaluated with the DSA.

The validity of the DSA was tested by comparing the predictions obtained with the DPM when defect states are assumed to be either amphoteric or decoupled in a-Si:H devices that are operating under different conditions: with and without bias light, under forward and reverse bias voltages, at several temperatures, for various intrinsic layer thicknesses, light source intensities, mobility gaps at the intrinsic layer, etc.

Figure 5 shows the *J–V* characteristic curves predicted by D-AMPS at room temperature using the DPM when DB are modeled with either amphoteric or decoupled states. The intrinsic layer of the a-Si:H p–i–n device was adopted 600 nm thick in agreement with the device of Fig. 2. On the right-hand axis of Fig. 5 the relative error $\varepsilon_{\text{AMP-DSA}}$ introduced by the DSA in the calculation of the current density J, is shown for different voltages V. Equation (7) was used to evaluate $\varepsilon_{\text{AMP-DSA}}$,

$$\varepsilon_{\text{AMP-DSA}} = 100\frac{J_{\text{AMP}} - J_{\text{DSA}}}{J_{\text{AMP}}}. \tag{7}$$

Under illuminated conditions and for reverse and low forward voltages (voltages close to the maximum power conditions), the error introduced by the DSA is caused by the higher recombination rate predicted by the DSA [20]. However, the relative error given by Eq. (7) remains below 0.5% in the device of Fig. 5 (600 nm intrinsic layer and at room temperature) and below 1.5% for all the devices that were analyzed (thicknesses between 200 and 2000 nm and temperatures between 250 and 400 K).

Under dark conditions and for forward voltages, the DSA predict the same current density at low voltages and slightly lower current densities at higher voltages than when DB states are assumed to be amphoteric. The errors become more visible for voltages near and below the knee of the *J–V* curve. In p–i–n devices with 2000 nm thick intrinsic layers, this discrepancy can reach values near 8% at room temperature. Differences are caused by the overestimation of the trapped charge inside the intrinsic layer by the DSA. Fermi quasi-levels are pushed closer to mid-gap by the DSA. Hence, the free carrier concentrations and the recombination rate become underestimated [20]. A thicker intrinsic layer has been intentionally adopted in order to weaken the electric field in the intrinsic layer and make our simulations more sensitive to the formalisms adopted to model the DB states.

When the band gap of the intrinsic layer is adopted 1.53 eV, scenario that corresponds to a-SiGe:H based p–i–n devices, the error shows the opposite sign, i.e., the current density predicted by D-AMPS with the DSA is greater than the one predicted with amphoteric states. For the mobility gap of 1.53 eV, the overestimation of the recombination rate predicted with the DSA does not significantly modify the free carrier concentrations as when the mobility gap in the intrinsic layer was assumed 1.72 eV and the final result is just a simple overestimation of the current density J (6–7% at the most).

Under dark conditions and for forward voltages, the error $\varepsilon_{\text{AMP-DSA}}$ is temperature dependent. The higher the temperature the greater the error becomes. For instance at 250 K and at 400 K, $\varepsilon_{\text{AMP-DSA}}$ reaches values near 2 and 5%, respectively, at low voltages where the current density J is controlled by recombination. At higher temperatures more electrons and holes are available for recombination and the difference between the DSA and the formalism of amphoteric states becomes more significant. The error $\varepsilon_{\text{AMP-DSA}}$ is lower at higher forward voltages where recombination does not entirely control the current density.

5 The Simmons–Taylor approximation with decoupled state applied to the defect pool model The DSA uses the SRH formalism to describe carrier trapping and recombination in acceptor-like and donor-like states. Simmons and Taylor have derived an elegant approximation of the SRH formalism that simplifies the calculation of the recombination efficiency and the trapped carrier concentrations for a continuous distribution of states [5]. They defined the intrinsic trap level, E_{T0}, as the energy where the emission rates of electrons to the conduction band and holes to the valence band are equal; i.e., $e_{\text{n}}(E_{\text{T0}}) = e_{\text{p}}(E_{\text{T0}})$. Since the emission rates exponentially increase or decrease with the trap energy E_{t}, either e_{n} or e_{p} can be neglected few kTs away from E_{T0}. Using this argument, the electron and hole occupation functions can be rewritten as

$$f^{\text{n}}(E_{\text{t}}) = \frac{n\sigma_{\text{N}}}{n\sigma_{\text{N}} + p\sigma_{\text{P}}}\left[1 + \exp\left(\frac{E_{\text{t}} - E_{\text{fnt}}}{kT}\right)\right]^{-1} \quad \text{for } E_{\text{t}} > E_{\text{T0}}, \tag{8a}$$

$$f^{\text{p}}(E_{\text{t}}) = 1 - f^{\text{n}}(E_{\text{t}}) = \frac{p\sigma_{\text{P}}}{n\sigma_{\text{N}} + p\sigma_{\text{P}}}\left[1 + \exp\left(\frac{E_{\text{fpt}} - E_{\text{t}}}{kT}\right)\right]^{-1} \quad \text{for } E_{\text{t}} < E_{\text{T0}}, \tag{8b}$$

where E_{fnt} and E_{fpt} are the quasi-Fermi levels for trapped electrons and trapped holes, respectively. The energies E_{fnt} (E_{fpt}) correspond to the energy levels E_{t} where a trapped electron (hole) has the same probability of being emitted to the conduction (valence) band than to recombine with a hole (electron) of the valence (conduction) band. Hence, E_{fnt} are defined as the energies where the conditions $e_{\text{n}}^0 = nv_{\text{th}}\sigma_{\text{N}}^0 + pv_{\text{th}}\sigma_{\text{P}}^0$ and $e_{\text{p}}^+ = nv_{\text{th}}\sigma_{\text{N}}^+ + pv_{\text{th}}\sigma_{\text{P}}^0$ are satisfied.

The occupation functions $f^{\text{n}}(E_{\text{t}})$ ($f^{\text{p}}(E_{\text{t}})$) are smooth functions of the gap state energy. They are approximately constant between the band edges and the quasi-Fermi levels for trapped electrons and holes where they show transitions steps [5]. Going from the valence toward the conduction band edge $f^{\text{n}}(E_{\text{t}})$ ($f^{\text{p}}(E_{\text{t}})$) decreases (increases) from 1 (0) to the pre-factor of Eq. (8a) (Eq. (8b)) around E_{fpt}, and from this pre-factor decreases (increases) to 0 (1) around E_{fnt}; being approximately constant between E_{fpt} and E_{fnt}. The recombination efficiency can be approximated by [5]

$$\eta_{\text{R}} = v_{\text{th}}\frac{\sigma_{\text{N}}\sigma_{\text{P}}np}{n\sigma_{\text{N}} + p\sigma_{\text{P}}}\left[1 + \exp\left(\frac{E_{\text{t}} - E_{\text{fnt}}}{kT}\right)\right]^{-1} \quad \text{for } E_{\text{t}} > E_{\text{T0}}, \tag{9a}$$

$$\eta_{\text{R}} = v_{\text{th}}\frac{\sigma_{\text{N}}\sigma_{\text{P}}np}{n\sigma_{\text{N}} + p\sigma_{\text{P}}}\left[1 + \exp\left(\frac{E_{\text{fpt}} - E_{\text{t}}}{kT}\right)\right]^{-1} \quad \text{for } E_{\text{t}} < E_{\text{T0}}. \tag{9b}$$

In these equations, only traps located between the quasi-Fermi levels for trapped carriers E_{fpt} and E_{fnt} are acting as effective recombination centers because outside of this energy range the probability of re-emission of electrons or holes to the conduction and valence bands, respectively, is higher than the probability of recombination.

In the Simmons and Taylor 0 K approximation, the electron occupation functions $f^{\text{n}}(E_{\text{t}})$ and $f^{\text{p}}(E_{\text{t}})$ and recombination efficiency are approximated by step functions as follows:

$$f^{\text{n}}(E_{\text{t}}) = \left\{\begin{array}{ccc} 1 & \text{for} & E_{\text{v}} < E_{\text{t}} < E_{\text{fpt}} \\ \dfrac{n\sigma_{\text{N}}}{n\sigma_{\text{N}} + p\sigma_{\text{P}}} & \text{for} & E_{\text{fpt}} < E_{\text{t}} < E_{\text{fnt}} \\ 0 & \text{for} & E_{\text{fnt}} < E_{\text{t}} < E_{\text{c}} \end{array}\right\}, \tag{10a}$$

$$f^{\text{p}}(E_{\text{t}}) = \left\{\begin{array}{ccc} 0 & \text{for} & E_{\text{v}} < E_{\text{t}} < E_{\text{fpt}} \\ \dfrac{p\sigma_{\text{P}}}{n\sigma_{\text{N}} + p\sigma_{\text{P}}} & \text{for} & E_{\text{fpt}} < E_{\text{t}} < E_{\text{fnt}} \\ 1 & \text{for} & E_{\text{fnt}} < E_{\text{t}} < E_{\text{c}} \end{array}\right\}, \tag{10b}$$

$$\eta_{\text{R}}(E_{\text{t}}) = \left\{\begin{array}{ccc} 0 & \text{for} & E_{\text{v}} < E_{\text{t}} < E_{\text{fpt}} \\ v_{\text{th}}\dfrac{\left(np - n_{\text{i}}^2\right)\sigma_{\text{N}}\sigma_{\text{P}}}{n\sigma_{\text{N}} + p\sigma_{\text{P}}} & \text{for} & E_{\text{fpt}} < E_{\text{t}} < E_{\text{fnt}} \\ 0 & \text{for} & E_{\text{fnt}} < E_{\text{t}} < E_{\text{c}} \end{array}\right\}. \tag{10c}$$

By replacing (9) in (4), the total recombination rate and the trapped charge density can be evaluated. The STA was conceived for forward biased devices, but it is interesting to check how the approximation behaves when the device is working under reverse voltages, the operating mode of optical detectors. In this paper, the accuracy of the STA were tested within the voltage range (−1 and 1.5 V) using as reference the *J–V* curves obtained with the DSA. 0KSTA were tested in the same voltage range under illuminated condition and only for forward voltage under dark condition using the same reference. The relative error $\varepsilon_{\text{DSA-STA}}$ introduced by the STA can be similarly defined $\varepsilon_{\text{AMP-DSA}}$ (see Eq. (7)) as

$$\varepsilon_{\text{DSA-STA}} = 100\frac{J_{\text{DSA}} - J_{\text{STA}}}{J_{\text{DSA}}}, \tag{11a}$$

where the meaning of the sub-indexes is straightforward. It is interesting to look also at the overall relative error made when the two approximations DSA and STA are simultaneously used, which is

$$\varepsilon_{\text{AMP-STA}} = 100\frac{J_{\text{AMP}} - J_{\text{STA}}}{J_{\text{AMP}}}. \tag{11b}$$

In Eq. (11b), the currents obtained with the DPM after both the DSA and the STA were applied and when DB are modeled as amphoteric states are compared at different device voltage. The errors defined in Eqs. (7) and (11) can be approximately related by (actually current densities in the denominators are different):

$$\varepsilon_{\text{AMP-STA}} \approx \varepsilon_{\text{AMP-DSA}} + \varepsilon_{\text{DSA-STA}}. \tag{12}$$

In the worst scenario, the relative errors will add but there are also some situations where a compensation effect between the two errors takes place and the total error is lower than the sum. It is important to remark that the STA and the 0KSTA apply to both defect states and tail states.

In Fig. 6, the *J–V* curves under AM1.5 illumination predicted by our computer code with the parameters of Table 1 are shown for four different cases: DB represented by amphoteric states, DB represented by decoupled states (DSA), defect and tail states approximated by the STA and defect and tail states approximated by the 0KSTA equations. In the first and second scenarios, tail states are modeled with the SRH formalism. The relative errors are shown at voltages below 0.82 eV. Very near V_{OC} the relative errors can be very large but meaningless because the current densities become very small. However, the spread predicted in V_{OC} with the four different models is not larger than 0.004 V.

Under illuminated conditions when either a reverse or a forward voltage is applied to the p–i–n device, the STA accurately reproduces the results obtained with the DSA. In Fig. 6, the *J–V* curves predicted with the STA and the DSA formalisms are on the top of each other. The error $\varepsilon_{\text{DSA-STA}}$ is below 0.001% for the voltage range under analysis. This

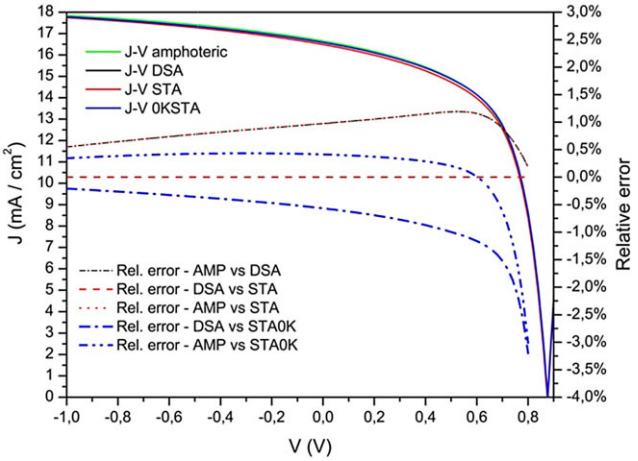

Figure 6 Predicted light *J–V* curves (under AM1.5 illumination) by D-AMPS for an a-Si:H based p–i–n device at room temperature using the AMP, DSA, STA, and 0KSTA formalisms. Relative errors are included. The intrinsic layer is 2000 nm thick.

result is expected because under illuminated conditions the quasi-Fermi levels for trapped carriers are far-off the intrinsic trap level E_{T0} what guarantees the exactness of the approximation [1]. Therefore, in this scenario the relative errors $\varepsilon_{\text{AMP-STA}}$ and $\varepsilon_{\text{AMP-DSA}}$ are quite similar. In other words under illuminated conditions, the error when the density of DB is modeled with the DPM is originated by the DSA.

Under dark condition and for forward biases, the STA shows also minor relative errors with respect to the DSA formalism (see Fig. 7). Only for very low-forward voltages; i.e., near the thermodynamic equilibrium condition, the $\varepsilon_{\text{DSA-STA}}$ becomes higher reaching figures between −4 and −7%. In this regime, the current density is controlled by recombination [21]. In this scenario, the quasi-Fermi levels

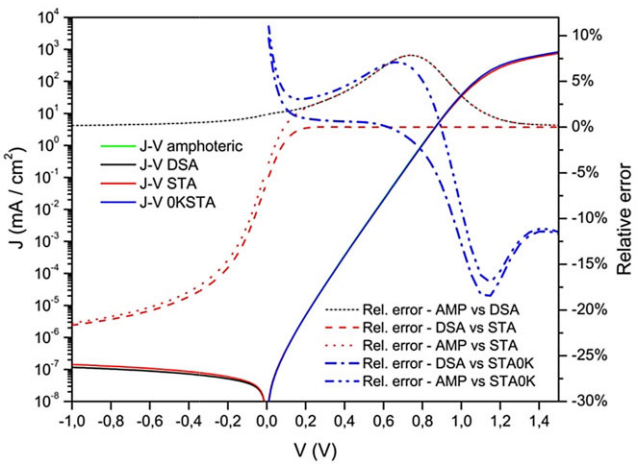

Figure 7 Predicted dark *J–V* curves by D-AMPS for an a-Si:H based p–i–n device using the AMP, DSA, STA, and 0KSTA formalisms. Relative errors are included. The intrinsic layer is 2000 nm thick and the temperature is 310 K.

for trapped carriers become close to the intrinsic trap level E_{T0} and the STA losses its accuracy. On the top of that the current density near thermodynamic equilibrium is very small favoring the appearance of higher relative errors.

Under dark conditions and for reverse voltages, the STA shows more significant discrepancies with respect to the DSA formalism. In this scenario, the current density is controlled by thermal generation of electron–hole (e–h) pairs [22, 23]. The energy positions of the quasi Fermi levels become inverted with respect to the ones obtained at forward biases. In other words, the electron quasi-Fermi level is below the intrinsic trap level E_{T0} and the hole quasi-Fermi level is above the intrinsic trap level E_{T0}. The quasi Fermi level for trapped holes is also above the quasi Fermi levels for trapped electrons inside the region of the intrinsic layer where thermal generation of e–h takes place.

Hence, the neglecting of either the electron or the hole emission coefficient under and above the intrinsic trap level E_{T0} become questionable [4]. However, the STA is still able to reproduce quite well the shape of the dark J–V curve at reverse voltages, but overestimating the current by less than 25% in all cases that were studied.

It is interesting to note that under dark conditions the relative errors $\varepsilon_{\text{DSA-STA}}$ and $\varepsilon_{\text{AMP-DSA}}$ have different signs. While the DSA formalism tends to underestimate the recombination rate [20] the STA tends to overestimate the same recombination rate [1]. Hence, there is compensation effect when the DSA and STA are simultaneously applied that reduces the overall relative error (see Eq. (11)).

When the device is subjected to forward voltages, the error $\varepsilon_{\text{AMP-STA}}$ is always lower than the error $\varepsilon_{\text{AMP-DSA}}$. Only for very low forward voltages ($V < 0.05$ V) this inequality is not true. Hence, unexpectedly the DSA in conjunction with the STA becomes a better approximation than the DSA alone. This difference is significant for forward voltages below 0.25 and 0.3 V and less important for higher forward voltages where the error $\varepsilon_{\text{AMP-STA}}$ remains lower than $\varepsilon_{\text{AMP-DSA}}$ but becoming quite similar. Only in the a-SiGe:H based p–i–n devices both $\varepsilon_{\text{DSA-STA}}$ and $\varepsilon_{\text{AMP-DSA}}$ show the same sign. In this case, both approximations tend to underestimate the recombination rate, the compensation effect is not taking place and the two errors add to each other.

The relative error $\varepsilon_{\text{DSA-STA}}$ does not show any sensitivity with respect to temperature in the range going from 250 to 400 K. On the other hand, $\varepsilon_{\text{AMP-STA}}$ changes with temperature due to the error introduced by the decoupled state approximation.

The relative errors $\varepsilon_{\text{DSA-STA}}$ and $\varepsilon_{\text{AMP-STA}}$ are also quite independent of the illumination intensity as long as the light flux is higher than $8 \times 10^{10}\,\text{cm}^{-2}\,\text{s}^{-1}$. For lower light intensities, the errors become more significant. The errors $\varepsilon_{\text{DSA-STA}}$ and $\varepsilon_{\text{AMP-STA}}$ can become higher than 15% when the light intensity is lower than $8 \times 10^{8}\,\text{cm}^{-2}\,\text{s}^{-1}$ when a reverse voltage is applied to the junction.

The 0KSTA also showed some interesting results. Under illuminated conditions for either reverse or forward voltages, there is a compensation effect between the errors introduced by the DSA and the 0KSTA. The DSA tends to overestimate the recombination rate while the 0KSTA tends to underestimate the same recombination rate. Hence, the current density loss predicted by applying both the DSA and the 0KSTA is lower than the current loss predicted by using only the DSA. The errors $\varepsilon_{\text{DSA-0KSTA}}$ and $\varepsilon_{\text{AMP-DSA}}$ remain approximately constant for different voltages and with an absolute value below 1.5% but they have different signs (see Fig. 6). If we conceive that the error introduced by both approximations (DSA and the 0KSTA) $\varepsilon_{\text{AMP-0KSTA}}$ as given by the algebraic sum $\varepsilon_{\text{AMP-0KSTA}} \sim \varepsilon_{\text{AMP-DSA}} + \varepsilon_{\text{DSA-0KSTA}}$ the overall error of making both approximations is near zero. Hence, the predicted current densities J are practically identical to the ones obtained with the DPM where DB are modeled as amphoteric states (see Fig. 6). Actually $\varepsilon_{\text{AMP-0KSTA}}$ is in absolute value below 0.5% for voltages below the maximum power point. Devices with a-SiGe:H intrinsic layers show a different type of behavior. At reverse voltages both $\varepsilon_{\text{DSA-0KSTA}}$ and $\varepsilon_{\text{AMP-0KSTA}}$ remain close of 0%. At forward voltages, the 0KSTA gives rise to higher current densities than the DSA. The error $\varepsilon_{\text{DSA-0KSTA}}$ increases in absolute value with the applied voltage and can reach values near -25% for voltages close and higher the maximum power point. When the forward voltage approaches V_{OC} the relative error naturally could become very high due to the very low current densities. In the 0KSTA, only the recombination processes through gap states located between the quasi Fermi levels for trapped carriers are accounted while the ones at gap states located outside of these energy levels are neglected (see Eq. (10c)). Hence, in p–i–n devices with low gap intrinsic layers where the recombination rate near the band edges is not negligible the 0KSTA tends to underestimate the recombination. When the applied voltage is increased the band edge profiles become more flat and the electric field weaker. This scenario gives rise to higher recombination rates and to increasing errors.

Under dark conditions and for reverse voltages, the 0KSTA cannot be calculated from Eqs. (10a)–(10c) that are no longer valid because the quasi-Fermi levels for trapped charges become inverted. Work is under progress to find new formulations of the 0KSTA in this case and we will concentrate here on the forward range when the device is the dark. Under dark conditions and for forward voltages but not too near the thermodynamic equilibrium ($V > 0.05$ V) the 0KSTA works within acceptable levels of errors (less than 8% in absolute value) at temperatures between 250 and 350 K in p–i–n device with intrinsic layers thinner than 800 nm. However, in quite thick devices like in p–i–n with 2000 nm intrinsic layers operating at room temperature (see Fig. 7) the error el $\varepsilon_{\text{DSA-0KSTA}}$ can reach values near -19%. The most significant errors in thick p–i–n devices can be observed for voltages between 0.8 and 1.3 V. When the forward applied voltage is increased within the range (0.8–1.3 V), the electric field changes its direction; i.e., the bands pass through the flat band condition. The magnitude of the electric field in the intrinsic layer bulk is weaker in thicker devices than in thinner samples. The weaker electric field

allows for higher recombination losses inside of the intrinsic layer. As it was already stated in the 0KSTA only the recombination processes taking place at gap states located between the quasi-Fermi levels for trapped carriers are accounted. This strong assumption neglects the recombination efficiency in gap states located outside of the quasi Fermi levels for trapped carriers but also tend to overestimate the recombination efficiency in gap states located inside of the quasi Fermi levels for trapped carriers (in the 0KSTA the recombination efficiency is assumed to be constant with respect to the gap state energy) where the most significant contributions to the recombination rate are present. These statements apply to p–i–n devices with a-Si:H intrinsic layers where the gap is higher than in the a-SiGe:H. On the top of that the DSA predicts more significant carrier trapping than the 0KSTA when the electric field is very weak (near zero). The magnified carrier trapping gives rise to the observation of a more pronounced band bending near the interfaces inside the intrinsic layer. This extra band bending makes more difficult the injection of free carriers into the intrinsic layer what in turn reduces the recombination losses. The final result of these two trends makes the DPM with the DSA to predict lower recombination rates and lower current densities than the DPM with the 0KSTA in the voltage range (0.8–1.3 V).

Under dark conditions and when forward voltages are applied, the error introduced by the 0KSTA is temperature sensitive unlike the one of STA. The error $\varepsilon_{\text{DSA-0KSTA}}$ increases with temperature. For instance in a p–i–n device with a 600 nm thick intrinsic layer at 250 K, the maximum error value is -0.5% and at 400 K is -12%. These errors are observed at low voltages where the current is controlled by recombination. At higher temperatures more states closer to the band edges contribute to the recombination rate while at lower temperatures states the near mid-gap take more control of the total recombination rate. At higher temperatures, the error $\varepsilon_{\text{DSA-0KSTA}}$ increases because the contribution of gap states outside of the quasi-Fermi levels for trapped carriers becomes not negligible (see Eq. (10c)).

Regarding the dependence of $\varepsilon_{\text{DSA-0KSTA}}$ with respect to the light intensity the 0KSTA is a good approximation for intensities higher than 8×10^{11} photons $\text{cm}^{-2}\,\text{s}^{-1}$ ($\varepsilon_{\text{DSA-0KSTA}}$ does not overcome 1%). On the other hand for intensities below 8×10^{9} photons $\text{cm}^{-2}\,\text{s}^{-1}$ $\varepsilon_{\text{DSA-0KSTA}}$ can be of the order of 20% when the p–i–n junction is reversed biased.

6 Conclusions The Simmons–Taylor approximation (STA) can be used in hydrogenated amorphous silicon (a-Si:H) and alloys based thin film devices when the density of DB is modeled with the defect pool model (DPM). The amphoteric nature of DB has to be approximated by two decoupled states (DSA) in order to test the STA when the recombination rate and the trapped charge density are evaluated. The current voltage under illuminated conditions can be accurately predicted by the STA for reverse voltages as long as the light intensity is not below 8×10^{10} photons $\text{cm}^{-2}\,\text{s}^{-1}$. The value of the relative error introduced by the approximation of amphoteric states by decoupled states does not overcome 1%. The same conclusions have been found to be valid for the SR curves.

Under dark conditions and forward voltages, the performance of the STA is also satisfactory. In a-Si:H devices for voltages higher than 0.05 V the error introduced by the combined use of the STA and the DSA is even lower than the error introduced by the DSA alone due a compensation effect occurring between the errors introduced by both approximations in the evaluation of the recombination rate. In a-SiGe:H based devices, the STA works also quite well although the compensation effect between the two errors does not take place. Under dark conditions and for reverse voltages, the STA preserves the shape of the current–voltage curve but overestimates the dark current by no more than 25% with respect to the currents obtained when DB are modeled as amphoteric states. Similar results with minor variations were obtained for different temperatures within the range 250–400 K. The errors can be higher in thick p–i–n devices than in thin p–i–n devices but they are still acceptable. Intrinsic layer thicknesses up to 2000 nm have been tested.

The 0 K Simmons–Taylor approximation (0KSTA) is also a useful tool that simplifies the modeling and the analysis of disordered semiconductor based devices but some precautions have to be taken into account. For a-Si:H devices under illuminated conditions (AM1.5 for instance), the use of the 0KSTA generates current voltage and SR with small errors as long as the applied voltage is below the one corresponding to the maximum power point. In contrast for a-SiGe:H devices, these errors become more significant when the characteristic curves are compared with their counterpart of the DPM assuming amphoteric-like defect states. The error obtained with the application of both the DSA and the 0KSTA is lower that the error obtained when only the DSA is applied due also to a compensation effect. Under low light level illuminated conditions, the relative error is still acceptable for light fluxes higher than 8×10^{11} photons $\text{cm}^{2}\,\text{s}^{-1}$. Under dark conditions and when forward voltages is applied the 0KSTA is accurate enough in p–i–n devices with intrinsic layer thicknesses below 800 nm and mobility gaps of 1.72 eV or higher, and within the temperatures range between of 250 and 350 K. In p–i–n devices where the intrinsic layer has a smaller mobility gap the accuracy of the 0KSTA is not as good as for a-Si:H or a-SiC:H intrinsic layers. The usual formulas for 0KSTA do not apply in under reverse bias and new approximate formulas have to be found to treat this regime.

Acknowledgements We highly appreciate the financial support of CONICET through the Grant PIP 112-201101-01052. We would also like to thank members of the department Photovoltaic Materials and Devices of Delft University of Technology, the Netherlands, for providing us of valuable experimental information.

References

[1] M. G. De Greef, F. A. Rubinelli, and R. van Swaaij, Thin Solid Films **540**, 227 (2013).
[2] J. Simmons and G. Taylor, Phys. Rev. B **4**, 502 (1971).
[3] A. Sturiale and F. A. Rubinelli, Thin Solid Films **516**, 7708 (2008).
[4] E. Klimovsky and A. Sturiale, Thin Solid Films **515**, 4826 (2007).
[5] J. Willeman, Ph.D. thesis, Delft University of Technology, Netherlands, 1998.
[6] M. J. Powel and S. C. Deane, Phys. Rev. B **48**, 10815 (1993).
[7] M. J. Powel and S. C. Deanne, Phys. Rev. B **53**, 10121 (1996).
[8] M. A. Kron and R. C. A. M. M. van Swaaij, Appl. Phys. **90**, 994 (2001).
[9] F. Rubinelli, J. Rath, and J. Schropp, J. Appl. Phys. **89**, 4010 (2001).
[10] G. Schumm, Phys. Rev. B **41**, 2427 (1994).
[11] C. Sah and W. Shockley, Phys. Rev. **109**, 1103 (1958).
[12] H. Okamoto and Y. Hamakawa, Solid State Commun. **24**, 23 (1977).
[13] F. Vaillant and D. Jousse, Phys. Rev. B **34**, 4088 (1986).
[14] C. Longeaud and J. P. Kleider, Phys. Rev. B **48**, 8715 (1993).
[15] C. van Berkel, M. J. Powell, and S. C. Deane, Non-Cryst. Solids **653**, 164 (1993).
[16] S. Olibet, E. Vallat-Sauvain, and C. Ballif, Phys. Rev. B **76**, 035326 (2007).
[17] J. Hubin, A. V. Shah, and E. Sauvain, Philos. Mag. Lett. **66**, 115 (1992).
[18] C. V. Halpern, Philos. Mag. B **54**, 473 (1986).
[19] W. Shockley and W. T. Read, Jr., Phys. Rev. **87**, 835 (1952).
[20] E. Klimovsky, J. K. Rath, R. Schropp, and F. Rubinelli, Thin Solid Films **422**, 211 (2002).
[21] F. Rubinelli, H. Liu, and C. Wronski, Philos. Mag. B **74**, 407 (1996).
[22] J. D. Cohen and D. V. Lang, Phys. Rev. B **25**, 5285 (1982).
[23] I. W. Archibald and R. A. Abram, Philos. Mag. **54**, 421 (1986).

